

Strengthening and toughening mechanisms in Mg–Zn–Y alloy with a long period stacking ordered structure

X.H. Shao^{a,b}, Z.Q. Yang^{a,*}, X.L. Ma^{a,**}

^a *Shenyang National Laboratory for Materials Science, Institute of Metal Research, Chinese Academy of Sciences, Shenyang 110016, People's Republic of China*

^b *Graduate School of Chinese Academy of Sciences, Beijing 100049, People's Republic of China*

Received 14 August 2009; received in revised form 24 March 2010; accepted 4 May 2010

Abstract

The deformation behavior and corresponding microstructure evolution of a $\text{Mg}_{97}\text{Zn}_1\text{Y}_2$ (at.%) alloy with a long period stacking ordered (LPSO) structure subjected to hot compression were investigated. The peak stress at 573 K was about 190 MPa, and no macroscopic fracture took place up to a strain of about 60%. The mechanisms responsible for the mechanical performance of the $\text{Mg}_{97}\text{Zn}_1\text{Y}_2$ (at.%) alloy are discussed based on microstructural investigations using various electron microscopy techniques. The high strength at elevated temperature could be attributed to synergetic strengthening refinement of the LPSO via kinking and a limited fraction of dynamical recrystallization. Microcracks nucleated at the interfaces in the sandwich structure composed of LPSO and nanometer thick Mg slices could weaken the alloy at late stages of deformation, but their propagation could be limited within the individual kink band where the microcracks nucleated, which could ensure the capability of the alloy to resist premature or catastrophic fracture. Furthermore, lack of deformation twins in Mg grains effectively reduced the potential nucleation sites for cracks, which should be another reason for the good ductility of the alloy. These findings may provide or evoke insights into methods for optimizing the mechanical properties of Mg alloys.

© 2010 Acta Materialia Inc. Published by Elsevier Ltd. All rights reserved.

Keywords: Mg–Zn–Y alloy; Long period stacking ordered structure; Kinking; Strengthening; Toughening

1. Introduction

Magnesium alloys are attractive as light weight structural materials owing to their low density, high specific strength, good damping and ease of recycling, which can be used in lots of areas, including automobiles, hand tools, sports equipment, electronic equipment and aerospace applications [1]. However, low strength and poor ductility hinder their widespread application. Therefore, great effort has been expended to improve the strength and ductility of Mg alloys.

Recently a new nanocrystalline $\text{Mg}_{97}\text{Zn}_1\text{Y}_2$ (at.%) alloy which exhibited a high thermal stability and superior mechanical properties with a tensile yield strength of ~ 600 MPa and elongation of $\sim 5\%$ at room temperature was produced by rapidly solidified powder metallurgy processing [2,3]. These excellent properties seem to originate not only in grain refinement but also a novel precipitate with a long period stacking ordered (LPSO) structure [4]. It was demonstrated that this phase is a long period chemical and stacking ordered structure by high angle annular dark field scanning transmission electron microscopy (HAADF STEM). Thereafter, various LPSO phases of 10H, 14H, 18R and 24R types have been observed in several kinds of ternary Mg–Zn–RE (rare earth) systems [5–8]. Notably, the formation of LPSO structure in Mg alloys was found to maintain the yield and ultimate

* Corresponding author.

** Corresponding author.

E-mail addresses: yangzq@imr.ac.cn (Z.Q. Yang), xlma@imr.ac.cn (X.L. Ma).

strength at 473 K at basically the same level as at room temperature [9], which was not observed in Mg alloys consisting of other kinds of precipitates. Therefore, Mg alloys containing an LPSO phase may be one potential structural material for elevated temperature applications. Some hardening or strengthening effects of the LPSO phase on Mg grains have been reported for Mg alloys containing LPSO structure. $\langle c + a \rangle$ dislocations were observed in Mg grains with LPSO precipitates, instead of $\langle a \rangle$ dislocations on the basal plane [10]. The result implies that the formation of an LPSO phase increases the critical resolved shear stress of the basal slip and activates non-basal slip in the Mg matrix, which is supported by first principle calculations [11]. Also, $\{10\bar{1}2\}$ deformation twins in the Mg matrix are prevented by the profuse LPSO phase in rapidly solidified $\text{Mg}_{97}\text{Zn}_1\text{Y}_2$ (at.%) alloys [12]. As for deformation of the LPSO phase itself, kink bands were observed within the LPSO structure in Mg–Zn–RE alloys [13–16]. Lately, Hagiwara et al. [13,14] reported that the plastic behavior of the Mg_{12}ZnY LPSO phase is highly anisotropic. Deformation kinks were initiated in the alloy and to some extent accommodated the compressive strain when stress was loaded parallel to the $(0\ 0\ 0\ 1)$ plane, in which case the Schmid factor for basal slip is negligible. They stressed that kink deformation is an essential mechanism to generate homogeneous strain in crystals and that it contributes to some extent to the ductility. However, the effect of kinking of the LPSO phase on the deformation behavior and mechanical properties of Mg alloys with LPSO structure is still unclear. Therefore, it is necessary to investigate the mechanism of deformation kinking in the LPSO phase in Mg alloys at the atomic level and, especially, its influence on the deformation behavior and mechanical properties of the Mg alloys. It is the aim of this study to reveal the microscopic mechanisms of the LPSO phase on strengthening and toughening of a $\text{Mg}_{97}\text{Zn}_1\text{Y}_2$ (at.%) alloy, which might shed new light on optimizing the mechanical properties of Mg alloys by distinctive microstructures.

2. Experiments

Samples with the nominal composition $\text{Mg}_{97}\text{Zn}_1\text{Y}_2$ (at.%) were prepared from high purity a Mg, Zn and Mg–25Y (wt.%) master alloy by high frequency induction melting in a graphite crucible at approximately 1023 K under an argon atmosphere. Specimens with the dimensions $4 \times 4 \times 8\text{ mm}^3$ were cut from the ingots by electrical discharge machining. Microhardness was measured in a MVK-H300 Vickers hardness testing machine, with a load of 50 g and a loading time of 10 s. Hot compression experiments were carried out at 573 K and a strain rate of $1.0 \times 10^{-3}\text{ s}^{-1}$ in a Gleeble-1500 thermal simulation machine. Prior to being compressed the specimens were conductively heated to 573 K at a heating rate of 5 K s^{-1} and held for 180 s for equilibration. The compression direction was parallel to the long axis of the specimens. Some tests were stopped when the specimens were deformed to

peak strains of $\sim 23\%$ and 60% without failure, then immediately water quenched to room temperature for microstructure analysis. The microstructures of the samples parallel to the compression axis were observed by scanning electron microscopy (SEM) and transmission electron microscopy (TEM). Thin foil samples for TEM were prepared by the conventional ion milling method. A Tecnai G² F30 microscope, operated at 300 keV and equipped with an HAADF detector, was used for microstructure analysis.

3. Results

3.1. True stress–true strain curve

The compression stress–strain curve of the $\text{Mg}_{97}\text{Zn}_1\text{Y}_2$ alloy under a strain rate of $1.0 \times 10^{-3}\text{ s}^{-1}$ at 573 K is shown in Fig. 1, which can be divided into three stages, OA, AB and BC. Initially the stress increased almost linearly in stage OA. In stage AB the stress continued to increase to a peak stress of about 190 MPa at a strain of about 23%, but the work hardening rate decreased continuously with increasing strain. Finally, the stress decreased slightly with increasing strain in stage BC, indicating a slight and slow work softening. The yield and peak stresses at 573 K were about 90 and 190 MPa, respectively. Samples with different applied strains (B, 23%; C, 60%) were selected for microstructural investigations, which hereafter are referred to as sample B and sample C, respectively.

3.2. Microstructure of $\text{Mg}_{97}\text{Zn}_1\text{Y}_2$ cast alloy

Fig. 2 is a back-scattered electron (BSE) SEM image of the $\text{Mg}_{97}\text{Zn}_1\text{Y}_2$ cast alloy, showing a duplex microstructure. The phase with bright contrast in the BSE SEM image was enriched in Zn and/or Y, compared with the dark contrast phase of the Mg matrix. The secondary phase, 5–35 μm in thickness, formed a three-dimensional quasi-continuous honeycomb-like network at Mg grain boundaries. The Mg

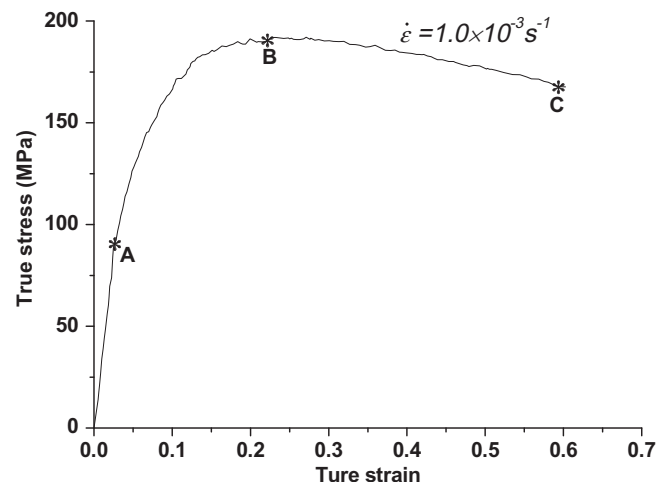


Fig. 1. True stress–true strain curves obtained from compression tests at 573 K under a constant strain rate of $1.0 \times 10^{-3}\text{ s}^{-1}$.

Download English Version:

<https://daneshyari.com/en/article/1447387>

Download Persian Version:

<https://daneshyari.com/article/1447387>

[Daneshyari.com](https://daneshyari.com)